

**SYNTHESIS AND CHARACTERIZATION OF ORGANIC-
INORGANIC FILMS BASED ON THE COMPOSITES OF
EPOXIDIZED NATURAL RUBBER (ENR-50)/POLYANILINE
AND ZIRCONIA**

by

MOHAMMAD HOSSEIN AZARIYAN

Thesis submitted in fulfillment of the requirements

For the degree of

Doctor of Philosophy

February 2016

DEDICATION

This thesis is affectionately dedicated to my dear mother, Manijeh Ataiee, for her constant love, encouragement and sacrifices, without, which I could not have been able to attain this level.

ACKNOWLEDGEMENTS

I take this opportunity to express my deepest appreciation and gratitude to my supervisor Professor Dr. Wan Ahmad Kamil Mahmood who has been a great mentor and a source of tremendous support for me. I would like to thank you for encouraging my research and for helping me grow as a research scientist.

I also express my sincere thanks to the lab assistants and other staff, including Mr. Kamarul, Mr. Ong, Mr. Azizo, Miss Ami and the late Mr. Burhanudin whose demise has been such a great loss to the School of Chemical Sciences. My special thanks go to Miss Jamilah, Mr. Johari, Mr. Masrul, Mr. Mutalib and Mr. Ikhvan from the Electron Microscope Department, School of Biological Sciences and the Archeology Center, Mr. Yushamdan from the School of Physics, Mr. Idzuan from the School of Mechanical Engineering and Miss Harry from the Science and Engineering Research Center (SERC). I am very grateful to all of them for their kind support and assistance during the data collection period of my PhD research. Additionally, I would like to thank Professor Dr. Ali Hossein Kianfar for his valuable comments and insights.

I am indebted to all my friends who have supported me over the last four years: Dr. Ali Salehabadi, Mr. Hossein Bahri, Mr. Amir Ehsan Torkamani, and Mr. Faisal Mohammad. Finally, my sincere words of thanks go to my dear family, though 'words' cannot express how grateful I am to my mother, my father and my beloved sister for all of the sacrifices they have made on my behalf. Especially, I owe much to my mother, Manije Ataiee, without whose love and understanding I would not have completed this work.

Mohammad Hossein Azarian

TABLE OF CONTENTS

	Page
ACKNOWLEDGEMENTS.....	II
TABLE OF CONTENTS	III
LIST OF TABLES.....	VIII
LIST OF FIGURES	X
LIST OF APPENDICES	XIV
LIST OF ABBREVIATIONS	XVI
GRAPHICAL ABSTRACT	XIX
CONCEPTUAL FRAMEWORK.....	XX
ABSTRAK.....	XXI
ABSTRACT	XXIII
CHAPTER 1– INTRODUCTION.....	1
1.1 Inorganic-Organic Composites.....	1
1.1.1 Application of IOCs.....	3
1.2 Problem statements.....	3
1.3 Significance of Study.....	4
1.4 Research objectives	4
1.5 Scope of the study.....	5
1.6 Organization of thesis	5
CHAPTER 2 – BACKGROUND AND LITERATURE REVIEW.....	7
2.1 Polyaniline	7
2.2 Polyaniline composites	8
2.2.1 Doping of polyaniline	12

2.2.2 Emulsion polymerization technique	12
2.3 Sol-Gel technique	13
2.4 Alkoxide precursors.....	16
2.5 Epoxidized natural rubber	17
2.6 Hybrids, composites and polymer blends	21
2.7 Chemical interaction in iocs	22
2.7.1 Thermal and spectroscopic evidents.....	24
2.7.1.1 Differential scanning calorimetric	24
2.7.1.2 Fourier transform infra-red spectroscopy	25
2.7.1.3 UV-Visible spectroscopy.....	26
2.7.1.4 X-ray photoelectron spectroscopy	27
CHAPTER 3 – MATERIALS AND EXPERIMENTAL METHODS.....	29
3.1 Chemicals and materials	29
3.1.1 Purification of ENR-50.....	29
3.2 Experimental procedures	29
3.2.1 Preparation of ENR-50/zirconia hybrid materials	29
3.2.2 Synthesis of Pani.DBSA.....	30
3.2.3 Preparation of ENR-50/Pani.DBSA composite films.....	31
3.2.4 Preparation of Pani.DBSA/zirconia hybrid materials.....	31
3.2.5 Preparation of ENR-50/Pani.DBSA/Zr ternary composite materials.....	32
3.3 Characterizations	32
3.3.1 Fourier transforms infra-red spectroscopy	32
3.3.2 Ultraviolet visible spectroscopy analysis	32
3.3.3 Scanning electron microscopy.....	33

3.3.4 Transmission electron microscopy	33
3.3.5 Refractive index measurement	33
3.3.6 Thermogravimetric analysis	33
3.3.7 Differential scanning calorimetry	34
3.3.8 Electrical conductivity measurement.....	34
3.3.9 X- ray Diffraction	35
3.3.10 Atomic force microscopy	35
3.3.11 Nanoindentation test	35
3.3.12 X-ray photoelectron microscopy	37
3.3.13 Gel permission chromatography.....	37
CHAPTER 4 – PREPARATION AND CHARACTERIZATION OF ENR-50/ZIRCONIA HYBRID FILMS	38
4.1. Interaction of zirconia on ENR-50	38
4.1.1. FTIR spectroscopy.....	38
4.1.2. UV–Vis spectroscopy	41
4.1.2.1 Optical transparency	45
4.2. Morphology of ENR-50/zirconia hybrid	47
4.3. Thermal behavior.....	50
4.3.1 Thermal gravimetric analysis	50
4.3.2 Differential scanning calorimetry	52
4.4 Refractive index.....	54
4.5 Summary.....	56

CHAPTER 5 – EPOXIDIZED NATURAL RUBBER (ENR-50)/ DODECYL BENZENE SULFONIC ACID DOPED POLYANILINE (PANI.DBSA) COMPOSITE FILMS	57
5.1 Interaction of ENR-50 and Pani.DBSA.....	57
5.1.1 Infrared spectroscopy analysis.....	57
5.1.2 UV Spectroscopy	61
5.2 Morphology	64
5.2.1 Scanning electron microscopy.....	64
5.2.2 Transmission electron microscopy	67
5.3 Thermal behavior.....	69
5.3.1 Thermal gravimetric analysis	69
5.3.2 Differential scanning calorimetry	72
5.4 Atomic force microscopy	74
5.5 Electrical conductivity of ENR-50/Pani.DBSA composites	77
5.6. Nanomechanical properties	79
5.7 Summary.....	81
CHAPTER 6 – PANI.DBSA/ZIRCONIA COMPOSITE CONDUCTING MATERIALS SYNTHESIZED BY SOL- GEL TECHNIQUE	82
6.1 Interaction of zirconia on Pani.DBSA.....	82
6.1.1 FTIR analysis.....	82
6.1.2 Effect of zirconium(IV)-n-propoxide on conductivity of Pani.DBSA	84
6.1.3 UV-Vis spectra and identification	85
6.2 Crystallinity study by X-ray diffraction analysis	88
6.3 Morphology	90
6.3.1 Scanning electron microscopy (SEM).....	90

6.3.2 Transmission electron microscopy (TEM)	92
6.4 Thermal behavior	93
6.4.1 Thermal gravimetric analysis (TGA)	93
5.4.2 Differential scanning Calorimetry	96
5.5 Summary	99
CHAPTER 7 – TERNARY COMPOSITES FROM EPOXIDIZED NATURAL RUBBER, POLYANILINE AND ZIRCONIA	100
7.1 Interaction of ENR-50/Pani.DBSA and zirconia	100
7.1.1 FTIR Analysis	100
7.1.2 X-ray photoelectron spectroscopy (XPS)	102
7.1.3. UV Spectroscopy	109
7.2 Morphology	110
7.2.1 Scanning electron microscopy	110
7.2.2 Transmission electron microscopy	112
7.3 X-ray diffraction patterns studies	115
7.4 Thermal behavior	116
7.4.1 Thermal gravimetric analysis	116
7.4.2 Differential scanning Calorimetry	118
7.5 Atomic force microscopy	120
7.6. Electrical conductivity	123
7.7 Nanoindentation properties	124
7.8 Summary	127
CHAPTER 8 – CONCLUSIONS AND FUTURE STUDIES	128
8.1 Conclusions	128

8.2 Future studies.....	133
REFERENCES	134
APPENDICES	147
Appendix A-Gel Permeation Chromatography (GPC).....	147
Appendix B-Fourier Transformed Infrared Spectroscopy (FT-IR).....	149
Appendix C-Nanoindentation Test.....	151
Appendix D-X-ray Photoelectron Spectroscopy	153
Appendix E-X-ray Diffraction.....	160
Appendix F- Thermal Gravimetric Analysis	163
Appendix G-Differential Scanning Calorimetry	164
Appendix H- Publications	166
LIST OF CONFERENCES	168
LIST OF PUBLICATIONS.....	169

LIST OF TABLES

		Page
Table 4.1	Characteristic FTIR bands of the ENR-50/zirconia hybrid films.	41
Table 4.2	Shift of wavelength of absorption peak due to $n-\pi^*$ transition of the nonbonding electron of the epoxide groups with the variation of zirconium(IV)-n-propoxide addition in the preparation samples, b-d.	44
Table 4.3	Refractive indexes of ENR-50 and its composition with zirconium(IV)-n-propoxide.	54
Table 5.1	Maximum degradation temperature and glass transition temperature of ENR-50, Pani.DBSA & EPD composites obtained from DTG and DSC analysis.	72
Table 5.2	Mean roughness (R_a) and root-mean square roughness (R_q) determined from AFM image for Polyaniline film and its blends with ENR-50.	75
Table 5.3	An average nanoindentation values for Pani.DBSA & EPD composites.	79
Table 6.1	Characteristic UV-Visible absorption peaks of Pani.DBSA and Pani.DBSA/Zirconia (PDZr) composites.	87
Table 7.1	Average nanoindentation values for Pani.DBSA & EPD composites.	125

LIST OF FIGURES

		Page
Figure 2.1	Emeraldine salt conversion to emeraldine base [20].	8
Figure 2.2	General sol-gel process reactions.	14
Figure 2.3	Molecular structure of epoxidized natural rubber.	17
Figure 4.1	FTIR spectra of ENR-50, ENR-50/zirconia and zirconium(IV)-n-propoxide. Spectrum (a) and (e) correspond to ENR-50 and zirconium(IV)-n-propoxide, respectively. The spectra of ENR-50/zirconia hybrid samples are presented by b, c and d.	39
Figure 4.2	Molecular structure of zirconium(IV)-n-propoxide.	40
Figure 4.3	UV-Vis spectra of ENR-50 and ENR-50/zirconia hybrid samples. Black color spectrum corresponds to ENR-50 while the spectra b, c and d represent the ENR-50/zirconia hybrid samples.	43
Figure 4.4	Possible mechanism of bonding between ENR-50 and zirconia.	45
Figure 4.5	The spectra of ENR-50 and its compositions with zirconia (10, 30 and 50 wt%) samples obtained for the higher wavelength range (200 to 800 nm).	46
Figure 4.6	Optical images of ENR-50/zirconia hybrid film samples prepared with 10 (a), 30 (b) and 50 wt % (c) of zirconium(IV)-n-propoxide.	47
Figure 4.7	SEM images of ENR-50/zirconia hybrid film samples (a), (b) and (c) obtained from 10, 30 and 50 wt% addition of zirconium(IV)-n-propoxide, respectively.	49
Figure 4.8	TGA curves of ENR-50 (a) and ENR-50/zirconia hybrid film samples (b, c and d).	51
Figure 4.9	DTG curves of ENR-50 (a) and ENR-50/zirconia hybrid film samples (b, c and d).	52
Figure 4.10	DSC heating scan curves of ENR-50 (a) and ENR-50/zirconia hybrid film samples (b, c and d).	53
Figure 4.11	Refractive indices of ENR-50 and ENR-50/zirconia hybrid films.	55
Figure 5.1	FTIR spectra of a) Pani.DBSA salt & b) ENR-50.	59

Figure 5.2	(a-e): FTIR spectra of (a) EPD1%, (b) EPD2.5%, (c) EPD5%, (d) EPD10% and (e) EPD20%.	60
Figure 5.3	Proposed hydrogen bonding formation between ENR-50 and Pani.DBSA salt.	61
Figure 5.4	UV-Visible spectra of a) ENR-50 b) Pani.DBSA.	62
Figure 5.5	Formation of anilinium-DBSA micelle and Pani.DBSA salt [135].	63
Figure 5.6	(a-e): UV-Vis spectra of (a) EPD 1% (b) EPD 2.5% (c) EPD 5% (d) EPD 10% (e) EPD 20%.	64
Figure 5.7	(a-f): SEM image of (a) Pani.DBSA film, (b) EPD 1%, (c) EPD 2.5%, (d) EPD 5%, (e) EPD 10%, (f) EPD 20%.	66
Figure 5.8	TEM image of (a) Pani.DBSA salt, (b) EPD 2.5%, (c) EPD 5%.	68
Figure 5.9	TGA/DTG curve of Pani.DBSA.	70
Figure 5.10	Thermo gravimetric curves of ENR-50 and EPD blend samples.	71
Figure 5.11	DTG curves of ENR-50 and EPD blend samples.	71
Figure 5.12	DSC heating scans curve of a) EPD 1%, b) EPD 2.5 %, c) EPD 5%, d) EPD 10% and e) EPD 20% at different amount of Pani.DBSA.	73
Figure 5.13	(a-e): Amplitude AFM images of Pani.DBSA(a),EPD 1%(b), EPD 2.5%(c), EPD 5%(d), EPD 10%(e).	76
Figure 5.14	Electrical conductivity of the ENR-50/Pani.DBSA composites as a function of weight ratio of Pani.DBSA content.	78
Figure 5.15	Load-displacement curves for a) Pani.DBSA, b) EPD 20%, c) EPD 10% and d) EPD 5%.	80
Figure 6.1	FTIR spectra of a) Pani.DBSA, b) PDZr 10%, c) PDZr 30%, d) PDZr 50%, e) PDZr 70% and f) zirconium(IV)-n-propoxide. Samples b,c,d and e were prepared by 10, 30, 50 and 70 wt% addition of zirconium(IV)-n-propoxide.	83
Figure 6.2	Proposed sol-gel reaction of zirconium (IV)-n-propoxide.	84
Figure 6.3	An electrical conductivity of the Pani.DBSA and Pani.DBSA /Zirconia composites as a function of weight ratio of zirconia content.	85

Figure 6.4	UV-Visible absorption spectra of a)Pani.DBSA, b) PDZr 10%, c) PDZr 30%, d) PDZr 50%, e) PDZr 70%.	87
Figure 6.5	XRD finger prints of a) Pani.DBSA, b) PDZr 10%, c) PDZr 30%, d) PDZr 50%, e) PDZr 70%.	89
Figure 6.6	SEM image of a) Pani.DBSA, b) PDZr 10%, c) PDZr 30%, d) PDZr 50% and e) PDZr 70%.	91
Figure 6.7	TEM images of a) Pani.DBSA, b)PDZr 30% and c)PDZr 70%.	93
Figure 6.8	Thermogravimetric curve of a) Pani.DBSA (PD), b) PDZr 10%, c) PDZr 30%, d) PDZr 50% and e) PDZr 70%.	95
Figure 6.9	DTG curve of PD and PDZr composites.	96
Figure 6.10	DSC heating scan curves of a) Pani.DBSA, b) PDZr 10%, c) PDZr 30%, d) PDZr 50% and e) PDZr 70% hybrid samples.	98
Figure 7.1	FTIR spectra of (a) EPD, (b) EPDZr10%, (c) EPDZr30%, (d) EPDZr50% and (e) zirconium (IV)-n-propoxide.	101
Figure 7.2	Proposed schematic illustrations for the formation of EPD & EPDZr composites.	102
Figure 7.3	XPS survey scans of (a) EPD, (b) EPDZr 10%, (c) EPDZr 30%, (d) EPDZr 50%. Inset shows the narrow scan of Zr3d.	105
Figure 7.4	C1s narrow scan spectra of a) EPD, b) EPDZr10%, c) EPDZr30% and d) EPDZr50%.	106
Figure 7.5	O1s narrow scan spectra of a) EPD, b) EPDZr10%, c) EPDZr30% and d) EPDZr50%.	106
Figure 7.6	O1s high depth deconvolution spectra of a) EPD, b) EPDZr10%, c) EPDZr30% and d) EPDZr50%.	107
Figure 7.7	C1s and Zr 3d high depth deconvolution spectra of a) EPD, b) EPDZr30%, c) EPDZr50%, d) EPDZr10%, e) EPDZr30% and f) EPDZr50%.	108
Figure 7.8	UV-Vis spectra of (a) EPD, (b) EPDZr10%, (c) EPDZr 30% and (d) EPDZr50%.	110
Figure 7.9	(a-d): SEM image of (a) EPD 2.5%, (b) EPDZr 10%, (c) EPDZr 30% and (d) EPDZr 50%.	112
Figure 7.10	TEM image of (a) EPD 2.5%, (b) EPDZr10%, (c) EPDZr30% and (d) EPDZr50%.	114

Figure 7.11	XRD pattern of a) ENR-50, b) Pani.DBSA, c) EPD 2.5, d) EPDZr 10%, e) EPDZr 30% and f) EPDZr 50%.	116
Figure 7.12	Thermo gravimetric curve of ENR-50, EPD and EPDZr composites with three different wt% of zirconium(IV)-n-propoxide.	118
Figure 7.13	DSC heating scans curve of a) ENR-50, b) EPD 2.5 %, c) EPDZr 10%, d) EPDZr 30% and e) EPDZr50%.	119
Figure 7.14	Topography (a-d) and corresponding phase images (a'-d') of a EPD composite film and its composition with different percentage of zirconium(IV)-n-propoxide (10,30,50) wt% obtained with tapping mode.	122
Figure 7.15	Electrical conductivity of the EPDZr composites as a function of weight ratio of zirconium(IV)-n-propoxide content.	124
Figure 7.16	Load-displacement curves for a) EPD, b) EPDZr 10%, c) EPDZr 30% and d) EPDZr 50%.	126

LIST OF APPENDICES

	Page
Appendix A-Gel Permeation Chromatography (GPC)	
Figure A1: The GPC result of ENR-50.	147
Figure A2: The GPC result of Pani.DBSA.	148
Appendix B-Fourier Transformed Infrared Spectroscopy (FT-IR)	
Figure B1: The FTIR spectra of ENR-50.	149
Figure B2: The FTIR spectra of Pani.DBSA.	149
Figure B3: The FTIR spectra of Zirconium n-propoxide.	150
Appendix C-Nanoindentation Test	
Figure C1: The Nano Test Indentation Review of Pani.DBSA.	151
Table C1: Details of nanonindentation test of Pani.DBSA.	152
Appendix D-X-ray Photoelectron Spectroscopy (XPS)	
Figure D1: XPS high depth deconvolution spectra of C1s in EPD composite.	153
Figure D2: XPS high depth deconvolution spectra of C1s in EPDZr10% composite.	154
Figure D3: XPS high depth deconvolution spectra of C1s in EPDZr30% composite.	155
Figure D4: XPS high depth deconvolution spectra of C1s in EPDZr 50% composite.	155
Figure D5: XPS high depth deconvolution spectra of O1s in EPD composite.	156
Figure D6: XPS high depth deconvolution spectra of O1s in EPDZr 10% composite.	156
Figure D7: XPS high depth deconvolution spectra of O1s in EPDZr 30% composite.	157
Figure D8: XPS high depth deconvolution spectra of O1s in EPDZr 50% composite.	157

Figure D9:	XPS high depth deconvolution spectra of Zr3d in EPDZr 10% composite.	158
Figure D10:	XPS high depth deconvolution spectra of Zr3d in EPDZr 30% composite.	158
Figure D11:	XPS high depth deconvolution spectra of Zr3d in EPDZr 50% composite.	159
Appendix E-X-ray Diffraction (XRD)		
Figure E1:	The XRD Fingerprints of ENR-50.	160
Figure E2:	The XRD Fingerprints of Pani.DBSA.	161
Figure E3:	The XRD fingerprint of zirconium dioxide (from instrument)	162
Appendix F- Thermal Gravimetric Analysis		
Figure F1:	The Thermogram of ENR-50.	163
Figure F2:	The Thermogram of Pani.DBSA.	163
Appendix G-Differential Scanning Calorimetry		
Figure G1:	The DSC of ENR-50.	164
Figure G2:	The DSC of Pani.DBSA	165
Appendix H- Publications		
Figure H1:	First publication (Third Chapter of the present thesis).	166
Figure H2:	Second publication (Fourth Chapter of the present thesis).	167

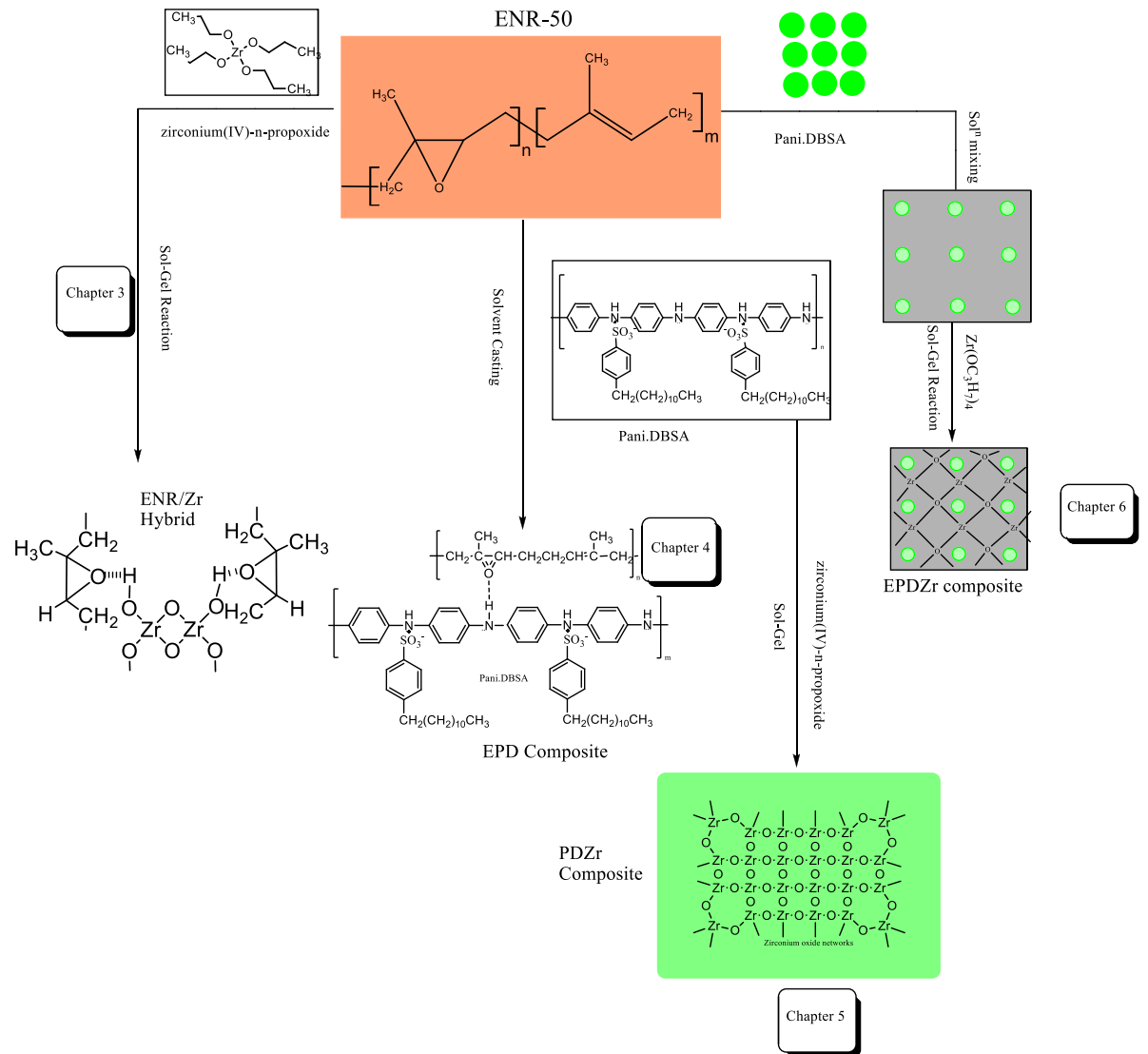
LIST OF ABBREVIATIONS

AFM	Atomic force microscopy
IOCs	Inorganic-Organic composites
IPNs	Interpenetrating polymer networks
RI	Refractive index
PT	Percolation theory
LED	Light emitting diodes
Pani	Polyaniline
ICPs	Intrinsically conducting polymers
DBSA	Dodecylbenzene sulfonic acid
CSA	Camphor sulfonic acid
PAN	Polyacrylonitrile
PES	polyethersulfone
TGA	Thermogravimetric analysis
XRD	X-ray diffraction
GPTMS	3-glycidoxypropyltrimethoxysilane
TEOS	Tetraethyl orthosilicate
THF	Tetrahydrofuran
ENR	Epoxidized natural rubber
ENR-50	Epoxidized natural rubber with 50% epoxidation
ACM	Acrylic rubber
PVA	Polyvinyl alcohol
BPA	Bisphenol A

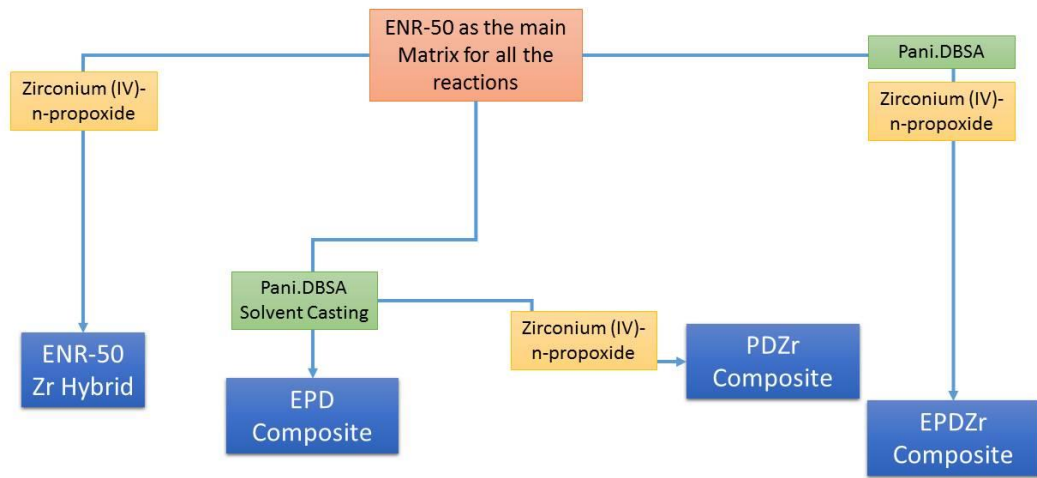
NR	Natural rubber
T _g	Glass transition temperature
GO	Graphene oxide
PCL	poly(ϵ -caprolactone)
PVP	Poly vinyl pyrrolidone
PAN	Polyacrylonitrile
EP	Epoxy resin
MMT	Montmorillonite clay
DSC	Differential scanning calorimetry
PU	polyurethane
FTIR	Fourier transform infrared spectroscopy
SMAA	Poly (styrene-co-methacrylic acid)
ES	Emeraldine salt
MWNTs	Multi-walled carbon nanotubes
GPTMS	3-glycidoxypropyltrimethoxysilane
XPS	X-ray photoelectron spectroscopy
NMR	Nuclear magnetic resonance
BE	Binding energy
KE	Kinetic energy
PS(OH)	poly(styrene-p-hexafluoro hydroxy isopropyl methyl styrene)
PVPy	poly(4-vinylpyridine)
PP	Polypropylene

PAMAM	polyamidoamine
PA6	Polyamide 6
MEL	Melamine
HDPE	High density polyethylene
HNTs	Halloysite nanotubes
APTES	3-aminopropyltriethoxysilane
APS	Ammunium persulfate
DBSA	Dodecylbenzene Sulfonic acid
EPD	ENR-50/Pani.DBSA
PDZr	Pani.DBSA/zirconia
EPDZr	ENR-50/Pani.DBSA-zirconia
RMS	Root mean square
SMFC	Semi metallic friction composites

GRAPHICAL ABSTRACT



CONCEPTUAL FRAMEWORK



**SINTESIS DAN PENCIRIAN FILEM ORGANIK-TAK ORGANIK
DARIPADA KOMPOSITE GETAH ASLI TEREPOKSIDA (ENR-
50)/POLIANILIN DAN ZIRKONIA**

ABSTRAK

Kandungan tesis ini memberikan tumpuan kepada penyediaan, sintesis dan pencirian komposit novel, iaitu bahan 'Komposit Tak organik-Organik' dengan sifat serta ciri yang telah dipertingkatkan. Getah asli terepoksida 50% (ENR-50) telah digunakan sebagai matriks polimer dan komposisinya bersama zirkonium (IV)-n-propoksida dan polianilin (Pani) telah dikaji. Pengikatan hidrogen yang telah menyumbang kepada pembentukan bahan komposit dapat dilihat melalui analisis kalorimetri dan pelbagai spektroskopi lain. Secara permulaannya filem hibrid ENR-50-zirkonia telah disintesis melalui kaedah sol-gel dengan mengubah kuantiti zirkonium (IV)-n-propoksida antara 10 hingga 50 wt%. Filem hibrid yang dihasilkan telah mempamerkan ketelusan optik yang sangat tinggi. Dengan penambahan 30 wt% zirkonium(IV)-n-propoksida, zarah-nano zirkonia telah diagihkan secara seragam dan homogen di dalam matriks ENR-50 dengan julat saiz zarah yang terdiri dari 50 hingga 70 nm. Bahan komposit baru dari ENR-50 dan Pani telah berjaya disediakan dengan menggunakan teknik tuangan pelarut. Anilin telah dipolimerkan dengan kehadiran asid sulfonik dodesilbenzene (DBSA). Seterusnya ia ditambah ke ENR-50 untuk penyediaan filem komposit ENR-50-Pani.DBSA (EPD). SEM (Mikroskop Elektron Imbasan) dan perkiraan nilai kekonduksian elektrik telah menunjukkan bahawa tahap-ambang serapan adalah pada kandungan 2.5 berat peratusan (wt%) Pani.DBSA. Data daripada peralatan 'nanoindentation' menunjukkan bahawa kekerasan (H) dan modulus Young (Es) meningkat dengan penambahan amaun polimer Pani.DBSA.

Pada bahagian ketiga, satu komposit baru Pani.DBSA/zirkonia (PDZr) telah berjaya disediakan dengan teknik sol-gel. Semasa kemasukan Zr (IV)-n-propoksida bahan komposit yang terhasil menunjukkan ciri-ciri kehabluran yang tinggi. Dalam pembentukan komposit PDZr, morfologinya berubah dan zarah-nano Pani.DBSA membentuk struktur rod dalam bahan komposit yang terhasil. Kekonduksian elektrik yang lebih tinggi telah diperolehi apabila komposit PDZr ditambah dengan 30% berat Zr (IV)-n-propoksida. Filem komposit ketiga daripada getah asli epoxidized (ENR-50), Pani.DBSA dan Zr(IV)-n-propoksida (EPDZr) telah direka melalui kaedah sol gel. Komposit EPDZr mempunyai nilai kekonduksian elektrik yang lebih ketara daripada komposit EPD pada amaun muatan Pani.DBSA yang sama. Kestabilan haba komposit EPDZr berkurangan disebabkan oleh kesan pemangkin ternari zirkonia. Analisis XPS telah digunakan untuk menyiasat kandungan permukaan komposit EPD dan EPDZr yang menyediakan pengetahuan lebih lanjut tentang interaksi diantara ENR-50, Pani.DBSA dan zirkonia. Bentuk bulat zarah yang besar bagi Pani.DBSA menjadi semakin kecil dengan kekasaran permukaan yang rendah dalam EPDZr 30 % dengan asas punca kuasa dua min 2 nm.

**SYNTHESIS AND CHARACTERIZATION OF ORGANIC-
INORGANIC FILMS BASED ON THE COMPOSITES OF EPOXIDIZED
NATURAL RUBBER (ENR-50)/POLYANILINE AND ZIRCONIA**

ABSTRACT

The current thesis focuses on the synthesis and characterization of novel Inorganic-Organic Composites (IOCs) materials with enhanced properties. Epoxidized natural rubber (ENR-50) was used as the polymer matrix and its composition with zirconium (IV)-n-propoxide and polyaniline (Pani) was investigated. The hydrogen bonding which contributes to the formation of the composite materials was observed by calorimetric and various spectroscopic analyses. Initially, ENR-50-zirconia hybrid films were synthesized through the sol-gel route by varying the amount of zirconium (IV)-n-propoxide ranging from 10 to 50 wt%. The prepared hybrid films exhibited very high optical transparency. With 30 wt% zirconium (IV)-n-propoxide addition, zirconia nanoparticles were uniformly and homogeneously distributed to the ENR-50 matrix with the particle sizes ranging from 50 to 70 nm. New composite materials from ENR-50 and polyaniline were successfully prepared using the solvent casting technique. Aniline was polymerized in the presence of dodecylbenzene sulfonic acid (DBSA). Subsequently it was added to ENR-50 for the preparation of ENR-50-Pani.DBSA (EPD) composite films. The SEM and electrical conductivity measurements revealed that the percolation threshold is at 2.5wt% of Pani.DBSA content. Nanoindentation results showed that the hardness and Young's modulus increased with higher additions of Pani.DBSA polymer. In the third part of the work, novel Pani.DBSA/zirconia (PDZr) composites were successfully synthesized using the sol-gel technique. Upon incorporation of Zr (IV)-n-propoxide the resulting composite

material showed greater crystallinity. Throughout the formation of PDZr composites the morphology changed and nanoparticles of Pani.DBSA formed rod-like structures in the resulting composite materials. A Higher electrical conductivity was obtained when the PDZr composite was incorporated with 30% weight of zirconium (IV)-n-propoxide. Eventually a novel ternary composite film composed of epoxidized natural rubber (ENR-50), Pani.DBSA and zirconium (IV)-n-propoxide (EPDZr) was designed taking a sol-gel approach. EPDZr composite has significantly higher electrical conductivity than EPD composite at the same loading of Pani.DBSA. The thermal stability of EPDZr composite decreased due to the catalytic effect of zirconia in ternary composites. XPS analyses were used to investigate the surface composition of EPD and EPDZr composites that provide further information about the interactions between ENR-50, Pani.DBSA and zirconia. The large spherical shape of Pani.DBSA becomes smaller with lower surface roughness in EPDZr30% with root mean square value of 2 nm.

CHAPTER 1

INTRODUCTION

1.1 Inorganic-Organic Composites

Inorganic-Organic Composite (IOC) materials are prepared or synthesized to seek new materials with improved properties. Organic polymers possess some limitations such as low thermal stability and poor mechanical, electrical and optical properties due to their intrinsic nature. Upon addition of inorganic materials their properties can be further improved and enhance their applications. On the other hand inorganic materials are usually known for their excellent thermal, electrical, optical and magnetic properties. Inorganic-organic composites (IOCs) can generally be prepared or synthesized by combining organic polymers and inorganic components in a chemical reaction. Inorganic metal alkoxides, which are usually used as the inorganic component, will form the inorganic part of the network in the IOCs. The interest to combine the properties of inorganic and organic components in order to create new composite materials has been a long time challenge to chemist, particularly material and inorganic chemist. It is noted that commercial IOCs have been part of the manufacturing industry since 1950s [1,2].

The classical high temperature solid-state reactions can no longer be used in the preparations of the IOCs due to the presence of organic components that have lower thermal stability as compared to inorganic glasses. Therefore a milder reaction condition is required for the formation of inorganic networks in IOCs. Sol-gel technique have been widely used by researchers to enable the preparation of organic polymer with inorganic materials at ambient temperature and low processing cost

[3,4]. Numerous reports can be found in the literature on the synthesis of IOCs in order to improve their morphology, thermal stability, conductivity and also to determine the structure and interactions between the components. Ochi et al. [5] prepared the epoxy resin and zirconia interpenetrating polymer networks (IPNs) via *in-situ* polymerization using zirconium alkoxide, where the use of zirconium alkoxide greatly influenced the morphology, optical transparency and refractive index (RI) of composite materials. IPNs can be prepared by synthesizing of inorganic component in a network form, normally by sol-gel technique in the presence of organic component without any covalent bonds between them. Vasudevan et al. [6], in the synthesis of titania and poly(vinyl pyrrolidone) nanocomposites have determined the structural properties and morphology of the prepared materials. The synthesis of other IOCs material such as carbon nanotube/rubber composites [7] and rubber/silica hybrids [8] have been reported to show how are the properties and applications of these new IOC materials.

Conventional conductive IOCs are typically a physical mixture of conducting materials such as metal or carbon powder distributed through the insulating polymer matrix [9]. The conductivity efficiency of these composites is governed by percolation theory (PT) [10]. PT can be used to understand the conductivity properties of the composites. Percolation threshold is the point that a conductive phase forming a continuous pathways through the polymer host matrix, which makes an electrons, be able to transport between conductive phases. There are many disadvantages related with these composites such as their high percolation threshold and their instability due to the heavy loading of the conducting particles. To overcome these draw backs recently IOCs of conducting polymers with elastomeric host polymer have been synthesized in order to increase the processability and improve the mechanical properties of these composites [11].

1.1.1 Application of IOCs

Individual polymers have a singular property profile capable of meeting only a limited number of applications. The application potentials for any polymer can be greatly enhanced by adding inorganic materials which resulted in the IOCs. The possible applications of the IOCs can be enormous. IOCs devices found application in electronic and optoelectronic sectors, which include photodiodes, solar cells, light-emitting diodes (LED), gas sensors and transistors [12,13]. Although most of these devices are able to be produced by fully polymer systems, the incorporation of the inorganic molecules in the polymer backbone will provide the composites with advantages such as durability and improved electronic properties.

Hence the combination of inorganic species with conducting polymers is yet another example of the potential of IOCs. Varieties of IOCs have already been prepared and show an interesting potential for magnetical, energy storage, catalytic, and electrochromic devices [14]. IOCs material have also been employed in several other fields such as dental applications, cancer therapy, drug delivery, implants, tissue engineering, body care and cosmetics [15].

1.2 Problem statements

- Organic polymers possess some limitations such as low thermal stability and poor mechanical, electrical and optical properties.
- The classical high temperature solid-state reactions can no longer be used in the preparations of the IOCs.

- Conventional Conductive IOCs have many disadvantages related with these composites such as their high percolation threshold and their instability due to the heavy loading of the conducting particles.

1.3 Significance of Study

The significance of this work is to provide brand new materials with enhanced properties and to determine their structure in order to give an explanation of the interactions of the components. IOCs have the capability to be developed as an interesting alternative to conventional inorganic or organic composites. Therefore, the development of new IOCs plays a crucial role in science and technology. Upon addition of inorganic materials within organic polymers, their properties can be further improved and their applications enhanced. However due to their low thermal stability, a milder reaction condition such as sol-gel technique is required for the formation of inorganic networks in IOCs. IOCs of conducting polymers – polyaniline with elastomeric host polymer i.e. ENR-50 – can be synthesized in order to have a lower percolation threshold and increase the process ability of these composites.

1.4 Research objectives

The main objective of this work is to synthesize novel inorganic-organic composites (IOCs), where the combined intrinsic properties of the inorganic and organic components are exploited:

- To explore new applications of epoxidized natural rubber (ENR-50) and investigate its probable interactions with zirconium oxide networks and polyaniline in the composite material in Chapter 4, 5 and 7.

- To investigate the thermal, surface, structural characteristics and morphology of the prepared IOC films in Chapter 4, 5, 6 and 7.
- To determine the influence of zirconia networks on the conductive properties of polyaniline in IOCs in the binary and ternary composite in Chapter 6 and 7 respectively.

1.5 Scope of the study

This research strives to portray the synthesizing of zirconia networks into polymer matrix composite materials. The polymer matrixes used in this study are epoxidized natural rubber with 50% epoxidation (ENR-50) and polyaniline due to their elasticity and conductivity properties respectively. The reactions were carried out by sol-gel and solvent casting techniques. In second part of the study polyaniline was synthesized in the presence of dodecyl benzene sulfonic acid and added to ENR-50 to prepare conductive polymer composite. The study mainly focuses on the interaction between organic and inorganic components and their resulting characteristic properties in the composites. Eventually effects of zirconia networks on the mechanical, thermal and electrical properties of ENR/Pani ternary composite were studied.

1.6 Organization of thesis

This thesis consists of seven (7) chapters. They are as follows:

- Chapter 1 provides a brief general introduction, problem statements, significance of the study, scope of the study, objectives and thesis layout.
- Chapter 2 provides background that covered literature survey and some important aspects in the field related to the other Chapters in the Thesis.

- Chapter 3 describes general information about the materials specification, equipments and experimental procedures used in this study.
- Chapter 4 describes the incorporation of zirconia oxide networks in epoxidized natural rubber by sol-gel technique.
- Chapter 5 provides the preparation and characterization of Epoxidized natural rubber/Pani.DBSA composite films.
- Chapter 6 describes the effects of zirconia network on the properties of the resulting Pani.DBSA composites.
- Chapter 7 describes the preparations and characterizations of the ternary composite films of ENR/Pani.DBSA with different amounts of zirconia loading.
- Chapter 8 provides a general conclusion that summarizes the main results and some recommendation for future works.

CHAPTER 2

BACKGROUND AND LITERATURE REVIEW

2.1 Polyaniline

The essential difference between electronically conductive polymers with those insulating polymers is that the former contain conjugated double bond while the latter do not. The polymer that possesses the electrical properties of a metal while maintaining its mechanical properties and processability is defined as ‘intrinsically conducting polymer’[16]. The presence of alternating single and double bonds in the polymer chain enable delocalization or mobility of electron along the polymer backbone. Hence, the conductivity is assigned by delocalization of π -bond electrons through the polymer backbone [17].

Polyaniline (Pani) has been around for a very long time, almost 180 years, and for last three decades, it has become as one of the most intensively studied conducting polymers [18]. Polyaniline is a phenylene based polymer with NH groups as its backbone. Aniline can be polymerized by oxidative polymerization in the presence of a protonic acid and oxidizing agent to form emeraldine salt (Es) which is a conducting version of polyaniline. Protonic acids role is not only to induce insulator to metal transition but also to act as a catalyst. On the other hand the synthesis of polyaniline is possible under acidic condition [19]. However as shown in Figure 2.1, Es can be rapidly converted to emeraldine base in an alkaline condition.

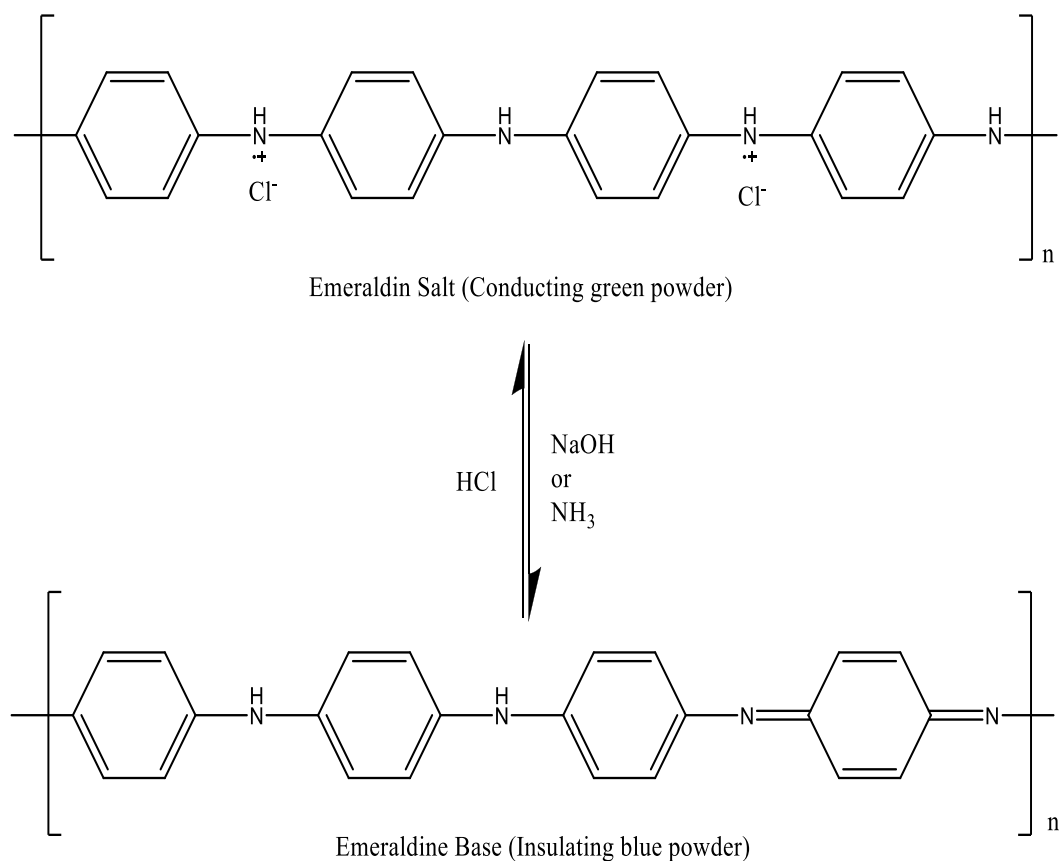


Figure 2.1: Emeraldine salt conversion to emeraldine base [20].

Polyaniline can be synthesized by chemical oxidative polymerization of aniline (such as: emulsion [18] and interfacial [21]), electrochemical polymerization [22], photochemically initiated polymerization [23] and enzyme-catalyzed polymerization [24].

Polyaniline has found a great potential for commercial applications in sensors [25], light-emitting diodes [26], solar cells [27], fuel cells [28] and transistors [29].

2.2 Polyaniline composites

The applications of Pani have not been fully utilized due to a number of limitations such as poor processability, low solubility and weak mechanical properties [30]. Numerous works have been carried out to overcome these weaknesses and one

such approach is the blending of Pani with processable thermoplastic polymers [31]. More recently, Pani was blended with commonly used polymers, in an effort to prepare conducting polymer composites. These composites showed that the primary structure of Pani is preserved to assure its conducting properties [32]. These Pani-polymer composites were designed to exploit the electrical conductivity of Pani and the physical properties of the polymer matrix. The resultant composites materials have offered numerous new applications in different fields, such as conducting membrane materials, sensor materials, and organic transparent electrodes [32,33]. Two synthetic methods can be employed to blend of polyaniline with the polymers, they are, (i) *in-situ* polymerization of aniline within the polymer matrix in the presence of doping agent and, (ii) addition of the doped Pani salt into the solution of polymer matrix. The latter is somewhat a preferred approach as described by several workers [34–36]. In these earlier work, Pani was initially doped with functional protonic acids such as, dodecylbenzene sulfonic acid (DBSA) or camphor sulfonic acid (CSA), in order that the conductivity properties of the Pani salts is preserved, while increasing its solubility in non-polar solvents. Pani doped with DBSA have been incorporated into commercial polymers such as polyacrylonitrile (PAN), epoxyresin and polyethersulfone (PES) [37–39].

Jianming et al. [40] have synthesized conductive composite fibers of polyaniline doped with dodecylbenzene sulfonic acid (Pani.DBSA) and polyacrylonitrile containing methylacrylate (Co-PAN) via a conventional wet spinning process. The influences of Pani.DBSA content on the electrical conductivity, thermal stability and mechanical properties of the composite fibers were investigated. The fiber with 7 wt% Pani.DBSA showed conductivity value of 10^{-3} S/cm. The thermal stability of the prepared composite fiber improved in both Co-PAN and Pani.DBSA.

Young et al. [41] have prepared blends of poly(butadiene-co-acrylonitrile) elastomer (NBR) and Pani.DBSA by solution mixing and casting method. The NBR-Pani.DBSA blends showed maximum electrical conductivities up to 10^{-2} S cm⁻¹. Blends prepared using NBR with the highest ACN content showed the best electrical properties with estimated percolation threshold at 6 wt% of Pani.DBSA content.

Jinzhang et al. [42] have prepared polyaniline/TiO₂ composite film deposited on the glass surface by sol-gel dip-coating technique and films were characterized using XRD, AFM, and UV-Vis. The average grain size of TiO₂ in the film was approximately 20 nm. After coating with Pani the particles were changed into irregular spherical-shaped and the size was increased up to approximately 35 nm in diameter.

Wei et al. [43] have reported the preparation of dodecylbenzene sulfonic acid-doped polyaniline (Pani.DBSA) with 3-glycidoxypropyltrimethoxysilane (GPTMS) through a sol-gel route without water and ethanol. Acetic acid was used to play both the roles of reagent and catalyst. M-cresol was also used as a secondary dopant in Pani.DBSA to enhance conductivity of hybrid films. The conductivity and visible light transmittance were varying with the molar ratio of acetic acid to GPTMS and m-cresol to GPTMS.

Olad et al. [44] have prepared ternary hybrid of Pani/epoxy/Zn nanocomposite as a thin layer coating (70 ± 5 um) on iron coupons and investigated their anticorrosion properties. Epoxy resin and zinc nanoparticles were applied as additives in the Pani matrix to improve the mechanical properties of Pani coatings. The synergetic effect of zinc nanoparticles and epoxy resin on the anticorrosive properties of conducting polyaniline coating was simultaneously investigated. The Pani/epoxy/Zn

nanocomposite coating showed the best anticorrosion performance by the application of 4 wt% zinc nanoparticles and 3–7 wt% epoxy resin.

Yu et al. [45] have prepared Pani/SiO₂ inorganic-organic hybrid films directly from polyaniline emulsion solution and Tetraethoxysilane (TEOS) by sol–gel process. The evolutions of phase, morphology and corrosion resistance ability of Pani/SiO₂ hybrid materials were investigated. It was demonstrated that Pani/SiO₂ hybrid films have a homogeneous and smooth surface without detectable cracks. However with the increase of TEOS content in Pani/SiO₂ hybrid materials tends to exhibit brittleness and micro-cracks which will lead to the deterioration of corrosion resistance ability.

Kumar et al. [46] have reported the preparation of DBSA doped polyaniline/multi-walled carbon nanotubes (DP/MWCNTs) nanocomposite by in situ oxidative polymerization. DP/MWCNTs was found to be an ideal adsorbent for the removal of Cr(VI) as compared to pristine and oxidized MWCNTs.

Jeong et al. [47] have explored the polymerization process for the fabrication of novel Pani/TiO₂ nanocomposite tubes. The strength of the prepared Pani/TiO₂ nanocomposite tubes for disinfection of microbial and chemical pollutants such as E. coli and methylene blue (MB) were investigated. Their research foundation showed that the synthesized nanocomposite tubes promises to be an effective hybrid material with multiple applications such as for wastewater treatment antifouling and an excellent antimicrobial agent.

Ashokan et al. [48] have prepared Pani/CuO hybrid composites by chemical synthesis method. The samples were characterized by structural, optical, morphological and electrical studies. FT-IR spectra of Pani/CuO hybrid composites shifted toward higher wave numbers compared with pure Pani. The band gap of Pani/CuO composites increased in compare with Pani that is due to the formation of

polaron as observed by UV-Vis spectra. The photoluminescence spectrum of nanoparticles showed a broad luminescence in green region, which indicates the possibility of these composites for developing of photonic devices.

2.2.1 Doping of polyaniline

The potential application of polyaniline was hindered by its disadvantages such as insolubility and low processability till important discovery of Cao et al. [49] who found that conducting polyaniline salts can be solubilized in organic solvent by the incorporation of surfactant acid such as camphor-10 sulfonic acid (CSA) or dodecylbenzene sulfonic acid (DBSA). As a result, it is possible to dissolve polyaniline in its fully doped state, into solvent such as chloroform, toluene and tetrahydrofuran (THF). In this method the solubility of polyaniline is forced by the long aliphatic hydrocarbon tail in the dopants while the sulfonate part forms an ionic bound with radical cation ^+NH sites of polyaniline chains. The solubility of polyaniline in organic solvents can also facilitate the preparation of conducting composites with various thermoplastic polymers to enhance the processability of polyaniline.

2.2.2 Emulsion polymerization technique

Emulsion polymerization is a type of free radical polymerization which involves emulsification of hydrophobic monomer by an emulsifier followed by the initiation reaction. The idea of using monomer in an aqueous suspension or emulsion system has been first discussed at the beginning of nineteenth century by Hofman and Delberuk as mentioned in a book of Chemistry and Technology of Emulsion Polymerization by van Herk [50]. Recently emulsion polymerization has been reviewed by Nomura et al. [51], Asua [52] and Chern [53].

Kima et al. [54] have successfully synthesized the emeraldine salt of polyaniline by a direct one step emulsion polymerization technique and showed that the molar ratio of the surfactant to aniline monomer affected the solubility and electrical properties of the final product. Kane & Krafcik [55], prepared nanostructured soluble conducting polyaniline salt by an emulsion polymerization technique and investigated the effects of both dopants and oxidant on material conductivity. Wua et al. [56] have synthesized polyaniline films via emulsion polymerization technique and showed that the prepared films display high sensitivity and high stability. Emulsion polymerization reactions have become more and more important technologically and commercially, as a method for producing high performance polymeric materials.

The main components of an emulsion polymerization are the monomers, dispersing medium (usually water), water soluble initiator and surfactant. A surfactant which also has been known as emulsifier, soap, or stabilizer, is a compound having both hydrophilic and hydrophobic segments. In emulsion polymerization, surfactants play three important roles: stabilization of the monomer, generation of micelle and stabilization of the growing polymer chains leading to stable end product.

2.3 Sol-Gel technique

There are several routes to prepare IOCs material, but the most prominent is by the sol-gel process which offers unique advantages such as: homogeneous multi-component system can be easily obtained, temperature required for material processing is considerably low and the rheological properties of the sol allows the formation of thin film, fiber and composite by different techniques such as dip coating, spinning and solvent casting [57].

The sol-gel process maybe can be define as the formation of metal oxide networks through polycondensation reactions of a precursor in a polymer solution liquid phase [58]. Sol is a suspension of particles of one phase in another major phase (polymer solution). When particles in a sol form continuous network, the sol loses its mobility and becomes a soft solid therefore the sol has formed gel.

The sol-gel process begins with a solution of metal alkoxide precursors $[M(OR)_4]$ and water, where M is a transition metal network-forming element, and R is an alkyl group. Hydrolysis and condensation of the alkoxide are the two fundamental steps to produce a network in presence of polymer matrix. The chemical reaction involved in the sol-gel process presented in Figure 2.2 [59].

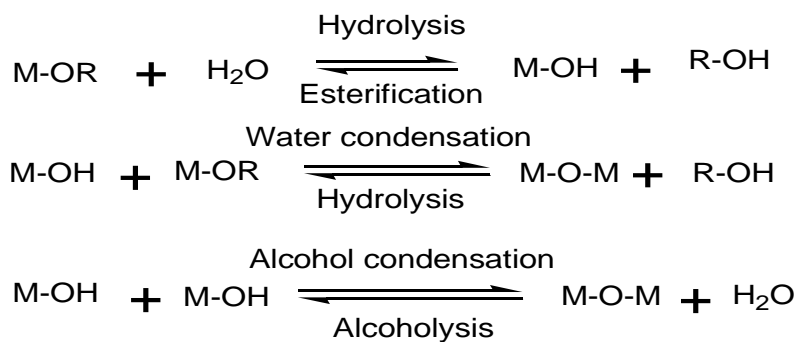


Figure 2.2: General sol-gel process reactions.

For the most transition metal oxide precursors the hydrolysis and condensation reactions are too fast which resulting in loss of morphological and structural control in the final oxide material. To overcome this problem the addition of water can be eliminated and reaction may carry out under reduced pressure [60].

The first sol-gel process began in 1845 by Ebelman [61], when he reported the formation of transparent material as a result of hydrolysis of an ester of silicic acid. Later in 1960's, Shroeder [62] deposited transparent coating on glass surface in order

to improve refractive index of glass by using thin layer of titanium butoxide as a precursor. Sol-gel science has been investigated extensively since the mid of 1970 till now when variety of IOCs formed from metal alkoxide solution [63].

Hashim et al. [64] have employed the sol-gel technique to prepare silica-reinforced vulcanizates using tetraethoxysilane (TEOS) and epoxidized natural rubber (ENR) and showed that under certain reaction conditions, the sol-gel vulcanizates obtained is more rigid and stronger than typical sulfur-cured ENR vulcanizate that contained comparable amount of silica. The stress-strain and dynamic mechanical property analysis suggested that the chemical bonds are formed between silica network particles and ENR polymer matrix.

Zareba-Grodz et al. [65] have synthesized an inorganic-organic hybrid by sol-gel process and found that the organic and inorganic phases were formed from two interpenetrating polymeric networks. The organic phase was a copolymer of acrylamide and 2-hydroxyethylmethacrylate while the inorganic phase was a silica polymer.

Bandyopadhyay et al. [66] have investigated the effect of polymer-filler interaction on solvent swelling and dynamic mechanical properties of the sol-gel derived acrylic rubber (ACM)/silica, and poly (vinyl alcohol) (PVA)/silica hybrid nanocomposites. Tetraethoxysilane (TEOS) at three different concentrations (10, 30, and 50 wt%) was used as the precursor for *in-situ* silica generation. In another publication he [8] reported the effects of various reaction parameters such as solvent, mole ratio of water to tetraethoxysilane and temperature on the structure and properties of epoxidised natural rubber/silica organic-inorganic hybrid nanocomposites. The sol-gel reaction was conducted at a constant concentration of tetraethoxysilane (45 wt% with respect to the rubber), used as the precursor for silica.

Ochi et al. [5] have prepared epoxy/zirconia hybrid materials using a bisphenol A (BPA) epoxy resin, zirconium (IV)-n-propoxide via *in-situ* polymerization. Both the sol-gel reaction and epoxy curing occurred simultaneously in a homogeneous solution, and organic–inorganic hybrid materials were obtained successfully. The zirconia networks produced by the *in-situ* polymerization were uniformly dispersed in the epoxy polymer matrix at the nanometer level. The hybrid materials obtained, exhibited excellent optical transparency. The heat resistance of the hybrid materials increased, and the refractive indices significantly improved with an increase in the zirconia content.

2.4 Alkoxide precursors

Metal alkoxides $M(OR)_4$ are enormously used in sol-gel chemistry owing to their ability to undergo hydrolysis and polycondensation reactions to create polymer oxide networks [67]. The chemical reactivity of metal alkoxide towards hydrolysis and condensation reactions highly depends on the electronegativity of the central metal atom and steric hindrance of the alkoxy groups (molecular structure of the metal alkoxides) [68]. Various Alkoxysilanes, such as tetramethoxysilane (TMOS) and tetraethoxysilane (TEOS) are widely used as metal alkoxide. However, other alkoxides such as aluminates, titanates, zirconates, and borates are also commonly used in the sol-gel process [69].

Zirconium is a multifunctional transition metal widely used in optical, electronic, magnetic and thermal environment [70]. Zirconium(IV)-n-propoxide was used as the precursor to produce zirconia networks. Its possess outstanding characteristics compared to TEOS, such as high ligand exchange rate [71], Lewis acidity [72] and high nucleophilicity of the alkyl group on zirconium. Therefore it is

widely used as precursor in the preparation of zirconia oxide network materials with a broad applications ranging from membranes, thin films, high refractive index material in multilayer optical coatings, thermal barrier coating, electronics and composites [73–76].

2.5 Epoxidized natural rubber

Epoxidized natural rubber (ENR) is a chemically modified natural rubber (NR) which the epoxide groups resulting from epoxidation, are randomly introduced to the polymer backbone [77]. Reacting natural rubber with peroxy formic acid can produce ENR which also called epoxidized cis-1,4-polyisoprene [78]. Figure 2.3 shows the chemical structure of ENR.

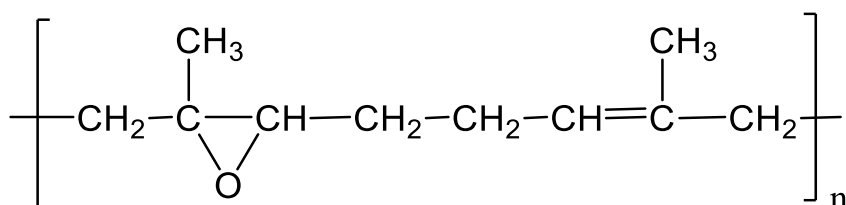


Figure 2.3: Molecular structure of epoxidized natural rubber.

Three types of ENR are commercially available; ENR 10, ENR 25 and ENR 50 where 10, 25 and 50 mole % of epoxide group incorporated into the natural rubber chain respectively. The properties of ENR change gradually with increasing epoxidation level. For instance, the glass transition temperature T_g goes up linearly as the level of epoxidation increases [79]. Owing to the polar nature of the oxirane groups, ENR demonstrates various interesting properties, e.g. low gas permeability or oil

resistance, as well as enhanced compatibility with other polymers [80,81]. Epoxidation of natural rubber can effects the polarity and glass transition temperature (T_g) of polymer. The polarity of ENR is proportional to mole % of epoxidation and increases with rise in epoxide contents. The glass transition temperature increases by approximately 1 °C for every 1 mole percent of epoxidation and from -60 for ENR-10 reaches to -25 for ENR-50. Epoxidized natural rubber can be tailored for various usages such as: tires, seals, coating and paints, cosmetic and adhesives [79,82,83]. Besides the commercial usage, ENR further has the potential to be applied as the polymer matrix in advanced materials [77,84,85].

Robertson et al. [86] have synthesized composites consisting of ENR and organically modified montmorillonite (OMON) in the ratio of 70:30 wt%. XRD measurements were made to estimate the basal plane spacing between the layered structures of the montmorillonite and its increment by 1.758 nm indicated that intercalation of ENR chains occurred in the silicate layers.

Lee et al. [84] have reported melt reaction in blends consisting of ENR-50 and poly(3-hydroxybutyrate) (PHB) by solvent-casting technique. Two-phase morphologies formed in the blends and two glasses transition temperatures observed at -18.4 °C and 1.2 °C, indicating that ENR-50 and PHB are immiscible polymers. After annealing at 190 °C an inward shift was observed and T_g gradually merging into a single transition indicating of change in miscibility of the polymers in blend.

Chuayjuljit et al. [87] have investigated the behaviors of epoxy resin blended with ENR with different epoxide contents (25, 40, 50, 60 and 70). The amounts of ENRs in the blends were 2, 5, 7, and 10 parts per hundred of epoxy resin (phr). It was found that the impact strength of epoxy resin could be improved by blending with

ENRs. While tensile strength and Young's modulus decreased with an increasing amount of epoxide groups and with an increasing amount of ENR in the blends.

Tanrattanakul et al. [88] reported the use of ENR as a toughening agent for nylon 6. Natural rubber (NR) was used to compare with ENR and polymer blends were prepared by using a twin-screw extruder. It was found that NR slightly decreased impact strength of nylon 6, whereas this property increased up to six fold by blending with ENR.

Pal et al. [89] have prepared ENR and organoclay nanocomposites by solution mixing method. The obtained nanocomposites were incorporated in NR and high styrene rubber (HSR) blends in presence of carbon black as reinforcing fillers. Morphology, curing characteristics, mechanical and thermal properties and wear characteristics of the nanocomposites were analyzed. The morphology of the ENR/nanoclay showed a highly intercalated structure. The overall mechanical properties and thermal stability was higher for the nanocomposites containing of carbon blacks.

Chang et al. [90] have prepared shape memory polymer networks from blends of ENR and end-carboxylated telechelic poly(caprolactone) (XPCL). The XPCL/ENR blends can form cross-linked structure by inter-chain reaction between the reactive groups of each polymer during molding at high temperature. Degree of crosslinking of the blend network and their thermo mechanical properties were characterized by gel content measurement, DSC and DMA. They also have found that the degree of crosslinking and crystalline melting transition temperatures was dependent upon the blend compositions as well as the molecular weight of the XPCL segment.

Moghadam et al. [91] have prepared ENR-50/regenerated cellulose (RC) blended films using an ionic liquid, 1-butyl-3-methyl imidazolium chloride (BMIMCl)

by casting solution method. The hydrogen bonding interaction between epoxy groups in ENR with hydroxyl groups of the RC in the blends were investigated by fourier transforms infrared (FTIR) spectroscopy. They have also found that crystallinity of the blends decreased moderately with the increase in ENR composition and thermal stability of RC significantly improved upon blending with ENR-50.

Mohammad et al. [92] have investigated the effect of mixing ratio on the properties of polypropylene (PP) incorporated with ENR. The blends of PP/ENR were prepared by melt compounding using an internal mixer. Mechanical testing such as tensile test, hardness test and impact test were performed to characterize the properties of PP/ENR blends. It was observed that the increase of the ENR percentage increases the toughness and flexibility of the PP/ENR blends. The changes were associated to the properties of the ENR elastic chains.

Tan et al. [93] have synthesized the nanocomposites of ENR and magnetite (Fe_3O_4). The Fe_3O_4 particles were incorporated *in-situ* in the presence of ENR to produce the various Fe_3O_4 /ENR nanocomposites. The X-ray diffraction analysis confirmed the existence of Fe_3O_4 particles in the composites; however, the FTIR and DSC studies indicated that there is no any chemical interaction between the particles and the polymer matrix.

Almaslow et al. [94] have prepared a group of semi-metallic friction composites (SMFC) consisting of epoxidized natural rubber–alumina nanoparticles (ENRAN), steel wool, graphite, and benzoxazine using a melt mixing method. The samples were subjected to mechanical and physical tests to determine the properties of the prepared SMFC. The addition of ENRAN contributed to the overall increase of hardness in the SMFCs. However, porosity was enhanced with higher ENRAN additions.

Xu et al. [95] have reported the use of ENR as an interfacial modifier to improve the mechanical properties of NR/silica composites. The ENR/Silica composite was prepared by using an open mill and the interfacial interaction of ENR with silica was investigated by FTIR, XPS, TEM, XRD and stress–strain testing. The results clearly indicated that the ring-opening reaction occurs between the epoxy groups of ENR chains and Si-OH groups of silica surfaces and the covalent bonds are formed. The bond formation can improve the dispersion of silica in the rubber matrix and enhance the interfacial combination between components.

Jo et al. [96] have prepared a nanocomposite consisting of ENR and functionalized multiwalled carbon nanotubes by eco-friendly melt blending method. Nanocomposites were found to exhibit greater thermal conductivity and excellent gas barrier properties. A maximum thermal conductivity was observed for nanocomposite obtained from 20% ENR and 3% wt% MWCNTs functionalized with aminosilane. Results indicated that the presence of epoxy moieties of ENR provided a stronger network formation between aminosilane treated MWCNTs surface and rubber matrices.

2.6 Hybrids, composites and polymer blends

The multicomponent polymer materials may include hybrids, polymer blends and composites that combined with other materials. According to Makishima [97] composites are mixture of materials consisting of matrix and micron-level dispersion while hybrids are sub-micron level mixture of two different kinds of materials. Hybrid materials can be broadly defined as nanocomposites with intimately mixed organic and inorganic components as mentioned by Sanchez [98]. According to the IUPAC recommendations as stated in IUPAC gold book, composite material defined as

“Multicomponent material comprising multiple, different (non-gaseous) phase domains in which at least one type of phase domain is a continuous phase”. However, nanocomposite defined as “Composite in which at least one of the phase domains has at least one dimension of the order of nanometers”. Furthermore hybrid material defined as “Material composed of an intimate mixture of inorganic components, organic components, or both types of component” [99]. The term polymer blend is used specifically to describe combination of two or more polymers that are not bonded chemically to each other [100]. Important combinations of two or more polymers bonded together include graft and block copolymer for instance. The term polymer composite is used originally to define combination of polymers with non-polymers such as graphene, clay and metal oxides. The ternary IOCs are used in material science by a broad spectrum of materials combinations.

2.7 Chemical interaction in IOCs

The primary differentiation of IOCs involves their phase behavior which can define as miscibility and compatibility versus phase separation. Miscibility in polymer composites is related to mixing of two polymer components at the molecular dimension scale which the properties observed are that expected of single material [101]. IOCs are considered immiscible if it is separated into phase comprised of the individual constituents. Immiscible polymer composites that exhibit macroscopically uniform physical properties can be considered as compatible materials. The macroscopically uniform properties are usually derived by chemical interactions between the components in the composite [102]. The advantage of compatible versus incompatible (no chemical reaction) is the IOCs property profile which is generally intermediate between the constituents.

The most common type of interaction studied in IOCs is hydrogen bonding. Hydrogen bonding as a particular interaction offers the ability to yield compatibility in polymer IOCs. Hydrogen bonding characteristically involves a bond between proton donor and proton acceptor groups. Polymers that represent the ability to hydrogen bond have been found to be compatible with a wide range of materials. Particular interactions such as hydrogen bonding between the inorganic phase and organic polymer host matrix are very important due to enhance the mechanical and thermal properties of resultant polymer composites as reported by Chan et al. [103].

She et al. [104] had synthesized epoxidized natural rubber (ENR)/ graphene oxide (GO) composite and found that ENR latex are assembled onto the surfaces of GO sheets by employing hydrogen bonding interaction as driving force which leads to the homogenous dispersion of GO within ENR matrix. The formation of hydrogen bonding between ENR and GO demonstrates a significant reinforcement for the ENR host.

The similar examples where hydrogen bonding interaction have been proposed to explain compatibility include, silica-reinforced tire composites compatibilized by using epoxidized natural rubber [79], epoxidized natural rubber/regenerated cellulose [91], poly(ϵ -caprolactone) (PCL)/ zirconium-propoxide (ZrO_2 matrix) [105], polyaniline/poly vinyl pyrrolidone (PVP)-polyacrylonitrile (PAN) [37,106] and polyaniline/ZnO [107]. A number of useful analytical and characterization methods have been developed for IOCs allowing for an improved understanding of the nature of the compatibility and their phase behavior.

2.7.1 Thermal and spectroscopic evidents

2.7.1.1 Differential scanning calorimetric

The calorimetric characterization of polymer composites can be done to investigate their compatibility. This instrument can determine specific heat, glass transition temperature, melting and crystallization point. The data can be obtained as a function of heating or cooling rate, and the sample temperature can be rapidly changed.

The characteristic transition of the amorphous polymers is the glass transition temperature. Below the glass transition temperature, the polymer chain is held in a random matrix, therefore is rigid and above the T_g rubbery behavior is observed. Single phase polymer composite will exhibit single and unique T_g , generally intermediate between the components value. The observation of a single T_g behavior for polymer composites has been well demonstrated in the literature [108–112]. The T_g determination, is an easy and effective method to evaluation of phase behavior.

Pan et al. [37] have prepared composites of polyacrylonitrile (PAN) copolymer containing 10% mass ratio methylacrylate and dodecylbenzene sulfonic acid doped polyaniline (Pani.DBSA) and DSC measurements revealed that there was only one T_g for each composite and the values of T_g varied with the content of Pani.DBSA, implying that the Pani.DBSA and PAN composites are compatible.

Jia et al. [113] have synthesized epoxy resin (EP) nanocomposites containing montmorillonite clay (MMT) and polyurethane(PU) and DSC data for the prepared nanocomposites showed two distinct T_g s which reveals the phase separation occurred. Both T_g increased and were systematically shifted towards each other with increasing MMT content which indicates that the MMT improved the compatibility between EP and PU. T_g results clearly showed that the presence of MMT led to a decrease in the